Nuclear Instruments and Methods in Physics Research A 622 (2010) 583–587

Contents lists available at ScienceDirect

Nuclear Instruments and Methods in Physics Research A

journal homepage: www.elsevier.com/locate/nima

Simulation of polyvinylidene fluoride detector response to hypervelocity particle impact

Andrew Poppe [a,b,c,*], Brian Jacobsmeyer [a,b], David James [a], Mihály Horányi [a,b,c]

[a] Laboratory for Atmospheric and Space Physics, 1234 Innovation Drive, Boulder, CO 80303, USA
[b] Department of Physics, University of Colorado, 2000 Colorado Ave, Boulder, CO 80309, USA
[c] Colorado Center for Lunar Dust and Atmospheric Studies, University of Colorado at Boulder, Boulder, CO 80303, USA

ARTICLE INFO

Article history:
Received 22 June 2010
Received in revised form
29 July 2010
Accepted 30 July 2010
Available online 5 August 2010

Keywords:
Polyvinylidene fluoride
Space dust instrumentation
Hypervelocity impacts
Crater scaling laws

ABSTRACT

Polyvinylidene fluoride (PVDF) films have been utilized as interplanetary dust detectors for many years in a variety of space environments. PVDF serves as a dust detector by producing a 'depolarization' charge upon hypervelocity impact. Previous instruments have relied on empirical calibrations to establish the relationship between the mass and velocity of the impacting dust particle and the generated charge. Here, we present a new theoretical derivation of PVDF response to non-penetrating hypervelocity particle impacts. We compare our simulation results to experimental calibration data from the Cosmic Dust Experiment on the Aeronomy of Ice in the Mesosphere satellite and the Student Dust Counter on the New Horizons mission. The simulation results agree well with the experimental data, yet suggest a modified crater diameter scaling law for non-penetrating hypervelocity impacts into PVDF.

1. Introduction

The use of polyvinylidene fluoride (PVDF) films as dust detectors was first conceived of by Simpson and Tuzzolino [1–6]. Simpson and Tuzzolino discovered that permanently polarized PVDF coated with a thin (≈ 1000 Å) layer of aluminum–nickel would produce a charge when impacted by a hypervelocity ($v > 1$ km/s) dust particle. They termed this charge 'depolarization' charge, distinguishing it from piezo- or pyroelectrically produced charges. Additionally, Simpson and Tuzzolino built a series of detectors and calibrated the depolarization charge against the mass and velocity of the impacting particle. These detectors (or variants thereof) flew on a number of missions, including: the DUst Counter and Mass Analyzer (DUCMA) instrument on Vega 1 and 2 [7], the SPAce DUSt (SPADUS) instrument on the Advanced Research and Global Observation Satellite (ARGOS) [8], the High Rate Detector (HRD) on the Cassini mission [9] and the Dust Flux Monitor Instrument (DFMI) on the Stardust mission [10]. Additionally, a nearly identical pair of PVDF instruments have flown as the Student Dust Counter (SDC) on the New Horizons mission [11] and as the Cosmic Dust Experiment (CDE) on the Aeronomy of Ice in the Mesosphere (AIM) mission [12]. These instruments have collected data on a variety of dusty phenomena, including the terrestrial micrometeorite flux [13,14], the plumes of Enceladus [15], dust ejection from the nuclei of Comet 81P/Wild2 [16] and Comet 1P/Halley [17] and interplanetary dust in the outer solar system [18]. PVDF detectors are an excellent device for in situ dust detection throughout the solar system, yet their fundamental response to hypervelocity dust impacts has not yet been thoroughly explained.

In this paper, we present a theoretical derivation of the behavior of PVDF detectors using experimental crater-scaling laws and a Poisson-relaxation simulation. In Section 2, we summarize the previous theoretical and empirical work concerning PVDF dust detectors. Sections 3 and 4 present our theoretical derivation of PVDF response and a comparison with previous experimental work, respectively. Section 5 discusses an adjustment to the crater diameter scaling law as suggested by our results. Finally, we conclude in Section 6.

2. Previous work

Simpson and Tuzzolino derived a simple theoretical expression for the response of permanently polarized PVDF films to hypervelocity dust impacts alongside their empirical calibration of the detectors [1,10]. They used the crater scaling equations developed in Ref. [19] and a simple electrostatics argument to calculate the change in charge on the aluminum–nickel layers after impact, assuming that the aluminum–nickel coating remained intact after the impact [1]. This resulted in an approximate power-law

* Corresponding author at: Laboratory for Atmospheric and Space Physics, University of Colorado at Boulder, 1234 Innovation Dr, Boulder, CO, 80303, USA.
E-mail address: poppe@lasp.colorado.edu (A. Poppe).

0168-9002/$ - see front matter © 2010 Elsevier B.V. All rights reserved.
doi:10.1016/j.nima.2010.07.088

dependence of the charge, Q, on the particle mass, m, and velocity, v, of $Q \propto m^a v^b$, with theoretical estimates for the exponents of $0.8 < a < 1.2$ and $1.8 < b < 2.6$. The empirical calibration of the 28 μm thick PVDF detectors yielded exponents, $a = 1.3 \pm 0.1$ and $b = 3.0 \pm 0.1$, somewhat different than predicted by theory. The authors acknowledged the difference and attributed it to a limited experimental dataset, rather than a possible deficiency in the theoretical derivation. Later work used empirical calibration data from SDC and CDE detectors to refine the earlier empirical fit, assuming the same power-law dependence on mass and velocity for the charge. The fit yielded exponents of $a = 1.052 \pm 0.004$ and $b = 2.88 \pm 0.06$ [20]. While based on a greater dataset than Simpson and Tuzzolino's work, the updated velocity exponent was outside the range originally predicted. Additionally, a satisfactory theoretical explanation for the generation of charge upon hypervelocity impact remained to be developed.

3. Theory of hypervelocity impact charge generation

We suggest that the source of the 'depolarization' charge created by permanently polarized PVDF films upon hypervelocity particle impact is the presence of fringing electric fields near the impact crater. After a dust particle impacts the PVDF, the aluminum–nickel layer above the crater is destroyed, exposing a portion of polarized PVDF (and thus, a net surface charge density) at the bottom of the crater. The exposed surface charge density creates an electric field that fringes around the remaining aluminum–nickel surface, changing the surface charge density of the plate near the impact crater. Fig. 1 shows a typical normalized potential contour of a cratered cross-section of PVDF, where the outward-bending potential contours near the impact crater indicate these fringing electric fields. The dimensions of the impact crater determine the strength of the resulting fringing fields and subsequently, the 'depolarization' charge.

Our solution of the potential distribution of a cratered PVDF detector uses a Poisson-relaxation method on a two-dimensional, 400×400 square grid with Dirichlet boundary conditions. As shown in Fig. 1, a cross-section of PVDF is modeled (depicted as the shaded portion), spanning the simulation area in one dimension. A typical crater is shown as the unshaded intrusion into the PVDF, where a constant crater width is assumed. Within the PVDF, the polarization and the relative permittivity are set to $P = 5 \times 10^{-2}\,\mathrm{C/m^2}$ and $\varepsilon_r = 12$, respectively, while areas outside the PVDF are set to vacuum. To determine the final potential distribution for a cratered PVDF detector, a standard grid relaxation method is used. Upon calculating the potential distribution, the surface charge density on the cratered aluminum–nickel plate is determined by calculating the change in electric field across the plate. Assuming azimuthal symmetry, the 'depolarization' charge is then given by the difference in the total surface charge before and after the impact.

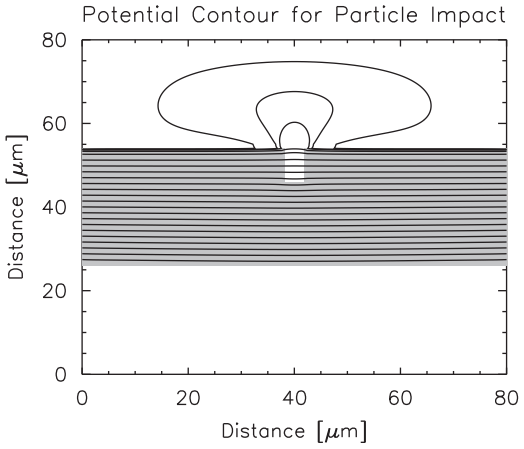

Fig. 1. A potential contour for a 1 μm radius particle impacting at 20 km/s. The shaded area represents intact PVDF material while the white rectangle above the bottom plate is the impact crater. Potential contours in the bulk of the PVDF are evenly spaced, while the frequency of contours near the upper surface is increased to qualitatively illustrate the fringing electric fields.

The dimensions of a dust particle's impact crater are determined by the characteristics of both the projectile and the target. As input to our simulation, we used independent scaling laws for the crater depth and diameter. The crater depth, f_c (cm), is given by [21]

$$f_c = 1.272 d_p^{1.056} \left(\frac{\rho_p}{\rho_{Fe}}\right)^{0.476} \left(\frac{\rho_{Al}}{\rho_T}\right)^{0.476} \left(\frac{\sigma_{Al}}{\sigma_T}\right)^{0.134} v^{0.806} \quad (1)$$

where d_p (cm) is the particle diameter, ρ_p (g/cm^3) is the particle density, ρ_{Fe} (g/cm^3) is the density of iron, ρ_{Al} (g/cm^3) is the density of aluminum, ρ_T (g/cm^3) is the target (PVDF) density, σ_{Al} (MPa) is the aluminum tensile strength, σ_T (MPa) is the target (PVDF) tensile strength and v (km/s) is the impact velocity. This formula was derived using previous crater depth scaling laws and new experimental data for iron projectiles impacting aluminum surfaces. Since no work has been done to explicitly derive crater scaling laws for iron grain impacts onto PVDF, we adapt an expression from Ref. [22] for the crater diameter, d_c (cm), for normal impact incidence:

$$d_c = 0.051 d_p v^{2/3} \quad (2)$$

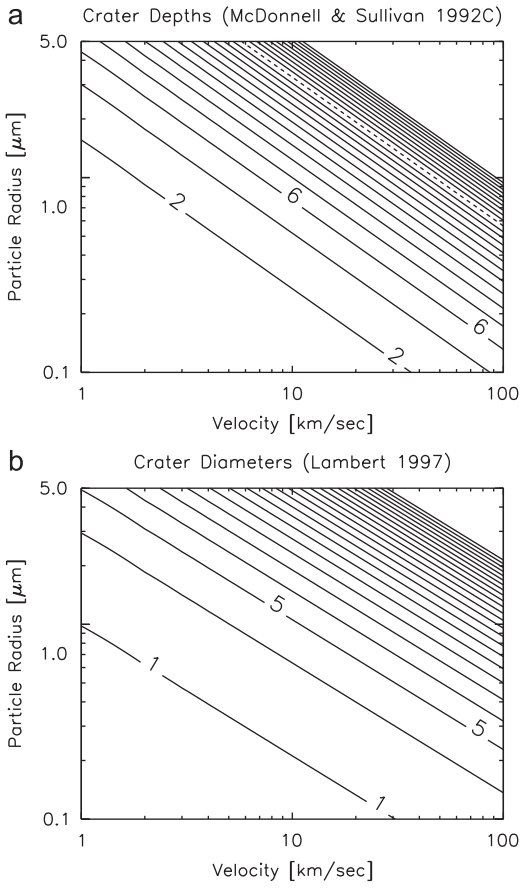

Fig. 2. Contour plots of crater depth and diameter. (a) Contour of crater depths using McDonnell's 1992C Equation. Depths, given in μm, are plotted against particle radius (μm) and particle velocity (km/s). Contours are evenly spaced every 2 μm; (b) contour of crater diameters using Lambert's 1997 Eq. (4). Impact hole diameters, given in μm, are plotted against particle radius (μm) and particle velocity (km/s). Contours are evenly spaced every 2 μm.

where d_p (cm) is the particle diameter and v (km/s) is the particle impact velocity. Contours of the crater depth and the crater diameter as a function of particle mass and velocity are plotted in Figs. 2(a) and (b), respectively.

As an additional comparison to the simulation, an analytic approximation can be formulated [23], assuming an infinite conducting plate with a circular hole in it and a distant source generating a constant electric field. The charge density, σ (C/m^2), is given as

$$\sigma = \frac{\varepsilon_0 E}{\pi}\left[\frac{a}{\sqrt{\rho^2 - a^2}} - \sin^{-1}\left(\frac{a}{\rho}\right)\right] \quad (3)$$

where E (V/m) is the background electric field, a (m) is the crater radius, ρ (m) is the radial distance from the center of the crater and $\rho > a$. Assuming azimuthal symmetry, the charge on the plate after impact can be calculated by integrating this function.

4. Comparison of simulations to experimental data

We simulated non-penetrating ($f_c < 28\,\mu$m, as the SDC and CDE PVDF detectors are 28 μm thick) dust impacts and compared the results to experimental charge measurements for the SDC and CDE PVDF detectors taken at the Heidelburg Dust Accelerator Facility [12]. Two runs were conducted at the Dust Accelerator Facility with only the acceleration voltage changed, in order to cover more of the m–v phase-space. As shown in Fig. 3 (with the two runs marked by either filled or unfilled symbols), dust impacts with masses (radii, with $\rho = 7.87\,$g/cm^3) ranging from approximately 10^{-12} g (0.31 μm) to 10^{-10} g (1.45 μm) and impact velocities from 2.5 to 11 km/s were simulated. Figs. 4(a)–(c) show the ratio of the simulated charge, Q_{sim}, to the experimental charge, Q_{exp}, as a function of the experimental charge for Simpson and Tuzzolino's theory [1], the analytic approximation [23] and this work. Typical error bars are indicated. Our simulation data agree more closely with the experimental data than both the analytic approximation and Simpson and Tuzzolino's theory, with most of the simulation data falling within a factor of two of the experimental data. However, all three theories exhibit a bias as a function of experimental charge, discussed in Section 5.

5. Adjusted crater diameter scaling law

Although the simulation shows an improvement over earlier theories, the bias against experimental charge deserves explanation.

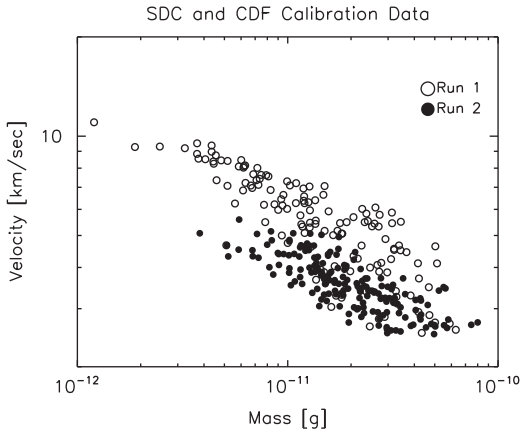

Fig. 3. The mass and the velocity of the two sets of calibration data taken at the dust accelerator at MPI-K in Heidelberg, Germany. Note that the two datasets were taken at slightly different accelerator energies.

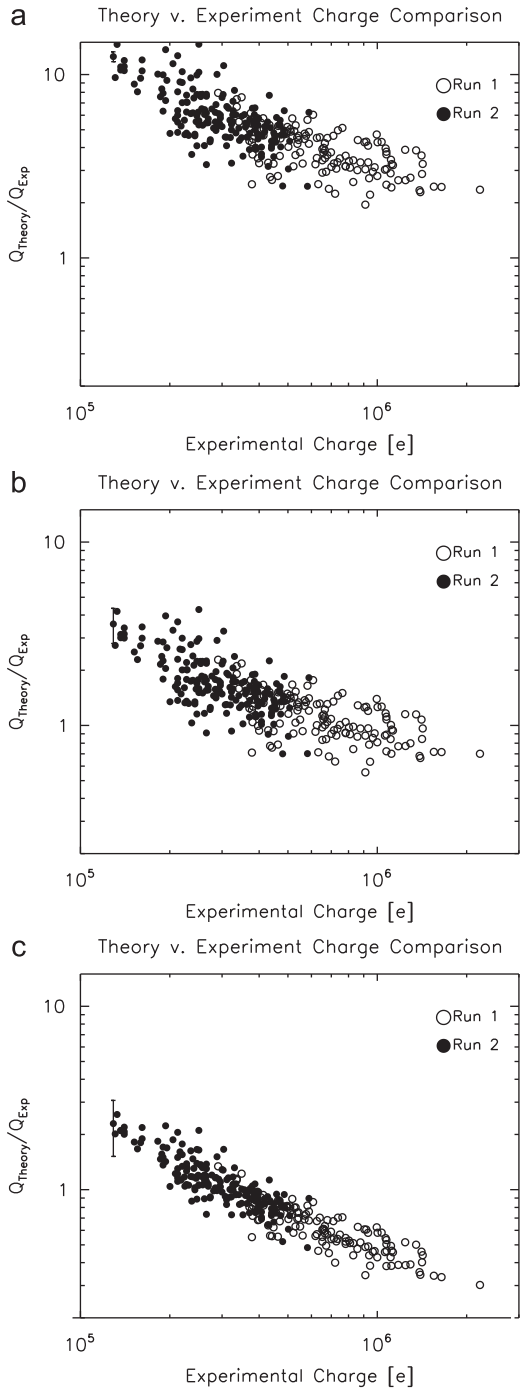

Fig. 4. The ratio of theoretical to experimental charge for (a) Simpson and Tuzzolino's theory, (b) an analytic approximation and (c) this work. Unfilled symbols are from Run 1 and filled symbols are from Run 2.

This work and Simpson and Tuzzolino's work both depend on the impact crater depth and diameter, yet the analytic approximation is only a function of crater diameter. Therefore, the bias exhibited in Fig. 4 is most likely due to the chosen diameter scaling law [22]. Using our simulation, we can derive a best fit diameter scaling law for iron particles onto PVDF by using a Monte Carlo approach. Previous work has shown that the crater diameter scales linearly with particle diameter [24]; therefore we assume a formula for the crater diameter, d_c, of

$$d_c = c d_p^{1.0} v^b. \quad (4)$$

Our method to determine the best fit diameter scaling law is to choose random doublets of {*b*, *c*}, recompute the simulated charge and compare this prediction to the experimental data. For each set of parameters, a goodness-of-fit value, χ^2, is calculated by

$$\chi^2 = \sum_j^N \frac{(Q_{exp,j} - Q_{sim,j})^2}{Q_{exp,j}}. \quad (5)$$

Smaller χ^2 values indicated a better fit with the corresponding doublet and by selecting the doublet with the lowest value, we can determine the best fit crater diameter scaling law. This process indicates that the best fit scaling law is given by

$$d_c = 0.019 d_p^{1.0} v^{1.35}. \quad (6)$$

Although this represents the best fit while keeping the diameter exponent fixed, this new law does not resolve the observed bias against experimental charge, as can be seen in Fig. 5. Thus, an additional diameter scaling law is derived, allowing the diameter exponent to change during the χ^2 analysis. This analysis results in a diameter scaling law:

$$d_c = 7.8 d_p^{2.14} v^{1.96}. \quad (7)$$

As Fig. 6 indicates, this new scaling law eliminates the previous bias, although with exponents that are significantly different from previous work [22,25].

6. Conclusions

A new theory has been proposed for the generation of charge from permanently polarized, aluminum–nickel coated PVDF films upon non-penetrating impact by hypervelocity particles. After impact, both the thin metal layer and a portion of the PVDF are destroyed, leaving an open impact crater with an exposed portion of polarized PVDF at the bottom. The presence of this polarization creates fringing electric fields at the crater opening and modifies the surface charge density on the aluminum–nickel layer. The change in surface charge density from before and after the impact leads to the observed charge.

This theory has been tested by developing a simulation to determine the potential distribution for a cross-section of a PVDF detector with a hypervelocity impact crater, where the relationship between particle mass and velocity and crater depth and diameter is taken from previous impact-crater scaling laws [21,22]. The potential distribution can be used to determine the electric field distribution and resulting surface charge density on the metal plates. We have compared our simulation results to calibration data taken for the Student Dust Counter and the Cosmic Dust Experiment [20] and found improved agreement from previous work.

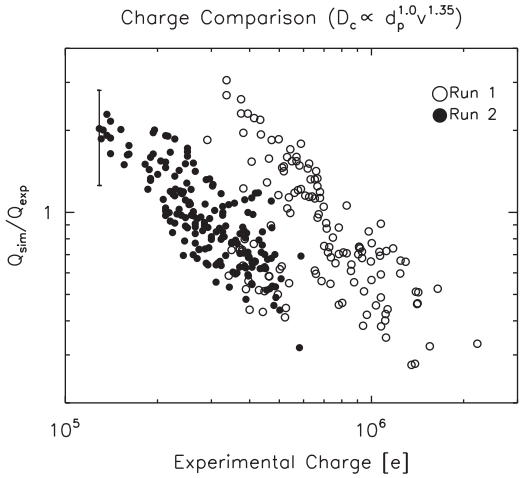

Fig. 5. The ratio of theoretical to experimental charge predicted by this work using Eq. (6) as the diameter scaling law. A typical error bar is also shown. The two bands of data are the two separate calibration datasets.

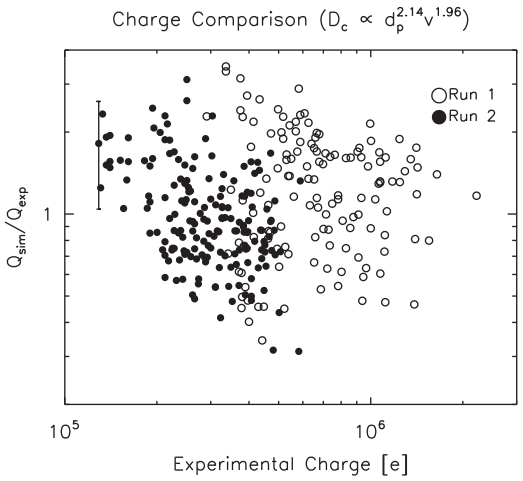

Fig. 6. The ratio of theoretical to experimental charge predicted by this work using Eq. (7) as the diameter scaling law. A typical error bar is also shown. Note that the two datasets do not have any bias with this scaling law.

Although our theory agrees well with the available experimental data, it exhibits a bias as a function of experimental charge. The bias was traced to the crater diameter scaling law used in the simulation. Using the simulation, a new diameter scaling law for non-penetrating impacts of iron particles onto PVDF targets is suggested. This new law corrects the experimental bias, yet is significantly different from previous cratering laws. Future experimental studies with the Dust Acceleration Facility at the Colorado Center for Lunar Dust and Atmospheric Studies (CCLDAS) of NASA's Lunar Science Institute should generate a better understanding of crater diameter scaling laws with PVDF targets. Additionally, future theoretical work is planned in order to develop a theory for the generation of charge upon penetrating hypervelocity impacts onto PVDF, where the charge scaling law is known to differ from that of penetrating impacts [10].

Acknowledgements

The authors thank E. Grün, M. Lankton, V. Hoxie, C. Bryant and S. Robertson for their contributions. The authors would also like to thank the staff at the Dust Accelerator Facility at the University of Heidelberg, Germany, especially E. Grün and R. Srama for their support. This research was funded by NASA through the Aeronomy of Ice in the Mesosphere and New Horizons missions.

References

[1] J.A. Simpson, A.J. Tuzzolino, Nuc. Instr. and Meth. Phys. Res. A 236 (1985) 187.
[2] J.A. Simpson, D. Rabinowitz, A.J. Tuzzolino, Nuc. Instr. and Meth. Phys. Res. A 279 (1989) 611.
[3] J.A. Simpson, A.J. Tuzzolino, Nuc. Instr. and Meth. Phys. Res. A 279 (1989) 625.
[4] A.J. Tuzzolino, Nuc. Instr. and Meth. Phys. Res. A 301 (1991).
[5] A.J. Tuzzolino, Nuc. Instr. and Meth. Phys. Res. A 316 (1992) 223.
[6] A.J. Tuzzolino, Adv. Space Res. 17 (12) (1996) 12123.
[7] M.A. Perkins, J.A. Simpson, A.J. Tuzzolino, Nuc. Instr. and Meth. Phys. Res. A 239 (1985) 310.
[8] A.J. Tuzzolino, et al., Planet. Space Sci. 49 (2001) 689.
[9] R. Srama, et al., Space Sci. Rev. 114 (2004) 465.
[10] A.J. Tuzzolino, T.E. Economou, R.B. McKibben, J.A. Simpson, J.A.M. McDonnell, M.J. Burchell, B.A.M. Vaughan, P. Tsou, M.S. Hanner, B.C. Clark, D.E. Brownlee, J. Geophys. Res. 108 (E10) (2003).
[11] S.A. Stern, Space Sci. Rev. 140 (2008) 3.

[12] M. Horanyi, et al., Space Sci. Rev. 140 (2008).
[13] A.J. Tuzzolino, et al., Planet. Space Sci. 49 (2001) 705.
[14] A.J. Tuzzolino, et al., Planet. Space Sci. 53 (2005) 903.
[15] F. Spahn, et al., Science 311 (2006) 1416.
[16] A.J. Tuzzolino, et al., Science 304 (2004) 1776.
[17] J.A. Simpson, et al., Nature 321 (1986) 278.
[18] A. Poppe, D. James, B. Jacobsmeyer, M. Horányi, Geophys. Res. Lett. 37 (2010).
[19] N. Pailer, E. Grün, Planet. Space Sci. 28 (1980) 321.
[20] D. James, M. Horányi, V. Hoxie, Rev. Sci. Instrum. 81 (2010).
[21] J. McDonnell, K. Sullivan, Hypervelocity impacts on space detectors: decoding the projectile parameters, in: Proceedings of the Workshop on Hypervelocity Impacts in Space. Unit for Space Sciences, University of Kent, Canterbury, U.K., 1991.
[22] M. Lambert, Adv. Space Res. 19 (2) (1997) 369.
[23] J.D. Jackson, Classical Electrodynamics, third ed., John Wiley and Sons, Inc, 1999.
[24] F. Hörz, D.E. Brownlee, H. Fechtig, J.B. Hartung, D.A. Morrison, G. Neukum, E. Schneider, J.F. Vedder, D.E. Gault, Planet. Space Sci. 23 (1975) 151.
[25] J.R. Baker, Int. J. Impact Eng. 17 (1995) 25.